Cofactor-Apoprotein Hydrogen Bonding in Oxidized and Fully Reduced Flavodoxin Monitored by Trans-Hydrogen-Bond Scalar Couplings

Frank Löhr,*[a] Gary N. Yalloway,[a, b] Stephen G. Mayhew,[c] and Heinz Rüterjans[a]

Hydrogen bonding plays a key role in the tight binding of the FMN cofactor and the regulation of its redox properties in flavodoxins. Hydrogen bonding interactions can be directly observed in solution by multidimensional heteronuclear NMR spectroscopy through the scalar couplings between donor and acceptor nuclei. Here we report on the detection of intermolecular trans-hydrogen-bond couplings (^{h}J) between the flavin ring system and the backbone of Desulfovibrio vulgaris *flavodoxin in the oxidized and the two-electron reduced states. For this purpose, experiments are adapted from pulse sequences previously applied to determining ^{h}J coupling constants in nucleic acid–base pairs and proteins. The resulting $^{h2}J_{N,N}$, $^{h4}J_{N,N}$, $^{h3}J_{C,N}$, and $^{h1}J_{H,N}$ couplings involve the $^{15}N(1)$, $^{13}C(2)$, and $^{15}N(3)$ nuclei of the pyrimidine moiety of FMN, whereas no such interactions are detectable for $^{13}C(4)$ and $^{15}N(5)$. Several long-range ^{15}N–^{15}N, ^{13}C–^{15}N, and ^{1}H–^{15}N J-coupling constants within the flavin are obtained as "by-products". The magnitudes of both ^{h}J and regular J couplings are found to be dependent on the redox state. In general, good correlations between ^{h}J coupling constants and donor-group ^{1}H chemical shifts and also crystallographic donor–acceptor distances are observed.*

Introduction

Flavoenzymes constitute a structurally and functionally diverse family of redox proteins.[1] The fact that they all share the flavin nucleus as the single redox unit to catalyze a wide range of biotransformations and electron-transfer processes implies that the redox properties are controlled by noncovalent interactions with the apoprotein. As the smallest members of the flavoprotein family, flavodoxins can serve as model systems for flavin-binding domains in order to provide insight into such interactions. They are small acidic flavoproteins that utilize riboflavin 5′-monophosphate (flavin mononucleotide, FMN) to transfer electrons between other redox proteins in a variety of microorganisms,[2] functioning at low redox potential close to that of the hydrogen electrode $E_{m,7} = -0.414$ mV. Their physical properties are well established, and their structures in all three accessible oxidation states have been extensively studied by X-ray crystallography[3] and solution NMR spectroscopy;[4] these revealed that tight, noncovalent binding of the cofactor results from stacking interactions of the isoalloxazine (flavin) ring system with aromatic side chains and from intermolecular hydrogen bonds (H-bonds). Flavodoxin-like structures occur as domains in certain larger redox proteins of higher organisms, such as cytochrome P450 reductase and NO synthase.

Flavodoxins are functionally equivalent to ferredoxins. In certain microorganisms they are synthesized in place of ferredoxin in response to iron deficiency,[5] while the sulfate-reducing bacterium *Desulfovibrio vulgaris*[6] produces flavodoxin even during growth on iron-rich media. In order to replace ferredoxin as an electron carrier in low-potential redox reactions, midpoint potentials of the cofactor must be strongly altered as a result of binding to the apoprotein. Hydrogen bonding is assumed to play a major role in this regulation.

A variety of NMR parameters, including reduced exchange rates of labile hydrogens,[7] $^{2}H/^{1}H$ fractionation factors,[7a,8,9] intramolecular[9] and trans-hydrogen-bond[10] ^{2}H isotope effects, isotropic[8d,11] and anisotropic[12] chemical shifts, ^{2}H quadrupolar coupling constants,[13] and scalar one-bond coupling constants[14,15] provide indirect evidence for the existence of H-bonding interactions. Direct "observation" of individual hydrogen bridges, however, is made possible by the presence of trans-H-bond scalar couplings, termed ^{hn}J, where n denotes the number of intervening bonds and h indicates that one of these is actually a H-bond. With the aid of COSY-type experiments, such electron-mediated, scalar couplings allow a correlation between magnetically active nuclei on both sides of the

[a] *Dr. F. Löhr, Dr. G. N. Yalloway, Prof. Dr. H. Rüterjans*
Institut für Biophysikalische Chemie
Zentrum für Biomolekulare Magnetische Resonanz
Johann Wolfgang Goethe-Universität
Marie Curie-Straße 9, 60439 Frankfurt am Main (Germany)
Fax: (+49) 69-798-29632
E-mail: murph@bpc.uni-frankfurt.de

[b] *Dr. G. N. Yalloway*
Current address:
Department of Biochemistry and Molecular Biology
University of British Columbia
Vancouver, British Columbia, V6T 1Z3 (Canada)

[c] *Prof. Dr. S. G. Mayhew*
Department of Biochemistry
Conway Institute of Biomolecular and Biomedical Research
University College Dublin
Belfield, Dublin 4 (Ireland)

 DOI: 10.1002/cbic.200400171 © 2004 Wiley-VCH Verlag GmbH & Co. KGaA, Weinheim

hydrogen bridge. Although the detection of two-bond couplings between amide protons and ^{113}Cd or ^{199}Hg, mediated by N–H···S hydrogen bonds in metal-substituted rubredoxin, had already been reported more than ten years ago,[16] the more recent discovery of $^{h2}J_{N,N}$ and $^{h3}J_{C,N}$ couplings in nucleic acids[17,18] and proteins,[19,20] respectively, demonstrated their general applicability to exploration of hydrogen-bond networks in biological macromolecules. Further types of trans-H-bond scalar couplings, such as $^{h1}J_{H,N}$,[18,21,22] $^{h4}J_{N,N}$,[23] $^{h2}J_{H,C'}$,[24,25] $^{h3}J_{H,C\alpha}$,[26] $^{h3}J_{H,H}$,[27] and $^{h3}J_{C\alpha,C'}$[28] have been observed subsequently. A comprehensive overview of the underlying NMR methodology, applications, and structure dependence of ^{h}J couplings has been presented in a series of reviews by Grzesiek and coworkers,[29] and developments in the field of ^{h}J-based NMR spectroscopy of DNA were summarized by Majumdar and Patel.[30]

While ^{h}J couplings within protein and nucleic acid molecules appear to be abundant, only a limited number of scalar couplings across intermolecular H-bonds in protein–ligand or nucleic acid–peptide complexes have been detected so far.[31–33] In a previous study[32] we examined the intermolecular hydrogen bonding pattern between oxidized *D. vulgaris* apoflavodoxin and the FMN phosphate group through $^{h2}J_{H,P}$ and $^{h3}J_{N,P}$ couplings. Here we focus on H-bond interactions involving the isoalloxazine ring system of the cofactor. It has been investigated whether N–H···N and N–H···O=C hydrogen bridges formerly inferred from crystallographic distances[3b,f,l,o] and from NMR chemical shift[15b,34] and NOE[4d,e,34] data can be detected in a more direct manner. The measurements required minor modifications to be introduced into experimental schemes previously applied to either protein or nucleic acid systems.

Results and Discussion

Flavins can occur in three distinct redox states: oxidized, one-electron reduced (semiquinone), and two-electron reduced (hydroquinone). For the flavodoxin from *D. vulgaris*, the midpoint redox potentials for the oxidized/semiquinone couple (E_2) and the semiquinone/hydroquinone couple (E_1) at pH 7.0 are shifted from −313 and −101 mV in free FMN[35] to −143 and −440 mV, respectively, upon binding to the apoprotein.[36] Unfortunately, NMR is unable to provide information about the immediate vicinity of the cofactor in the semiquinone form, due to the compound's radical character, which causes severe line broadening. There is, however, evidence from X-ray crystallography that the FMN–apoprotein contacts are very similar for the one- and two-electron reduced species of flavodoxins.[3f,k] This study of H-bonding interactions therefore concentrates on the oxidized and the fully reduced forms of the flavin, depicted in Scheme 1.

The cofactor binding site is primarily formed by three polypeptide loops near the surface of the protein. Intermolecular hydrogen bonding networks involving the isoalloxazine part of FMN in both redox states are represented in Figure 1. The most obvious difference is a reorientation of the Gly61-Asp62 peptide, enabling the formation of a H-bond between the N(5) nitrogen of reduced FMN and the carbonyl oxygen of Gly61,

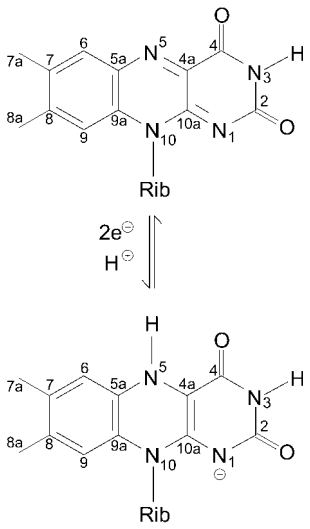

Scheme 1. *Chemical structures and numbering scheme of the oxidized (top) and fully reduced (bottom) forms of the isoalloxazine ring system of FMN, which can be interconverted by a two-electron transfer. Rib denotes the ribityl phosphate ($-CH_2(CHOH)_3CH_2OPO_3^{2-}$) side chain.*

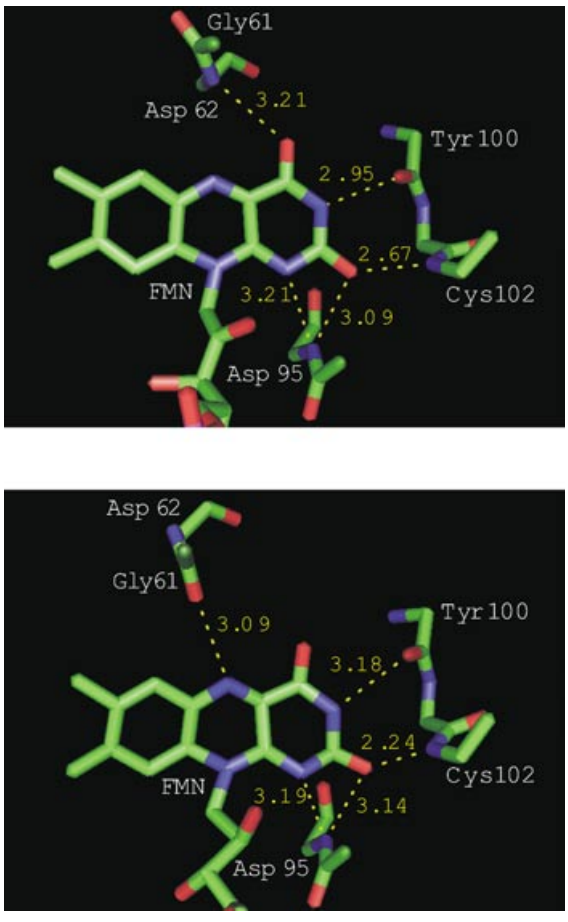

Figure 1. *Stick representation of the flavin-binding site in oxidized (top) and fully reduced (bottom)* Desulfovibrio vulgaris *flavodoxin. Only backbone atoms of apoprotein residues potentially involved in hydrogen bond interactions with the isoalloxazine ring of the cofactor are drawn. Relevant N(–H)···N and N(–H)···O distances are in Å. The figure was prepared by using PyMOL[37] with the low-temperature (−150 °C) X-ray coordinates of Watt et al.[3f]*

 © 2004 Wiley-VCH Verlag GmbH & Co. KGaA, Weinheim

while the H-bond between the nitrogen of Asp62 and the FMN C(4) carbonyl is broken. The hydrogen bonds between the N(1)–C(2)O–N(3)H moiety of the flavin ring and residues Asp95, Tyr100, and Cys102 are believed to exist in both redox states.

In order to detect cofactor–apoprotein hydrogen bonds of *D. vulgaris* flavodoxin in solution directly, a variety of quantitative *J* correlation[38] experiments were carried out. These 1) allow identification of a H-bond interaction by correlating the chemical shift of the involved proton with those of the donor ^{15}N and the acceptor ^{15}N or ^{13}CO nuclei, and 2) provide a measure of its strength through the magnitude of the trans-H-bond scalar coupling.

Measurement of $^{h}J_{N,N}$ coupling constants

Homonuclear ^{15}N–^{15}N couplings were detected through a [^{15}N,^{1}H]-TROSY-HNN-COSY experiment.[17] This "out-and-back"-type correlation scheme yields in-phase diagonal and cross-peaks of opposite sign. Their intensity ratio depends on the magnetization transfer times Δ employed and on the magnitude of the active coupling constants according to $-I_{cross}/I_{dia} = \tan^2(\pi J\Delta)$, which can be exploited for a quantitative determination of the latter. In a preliminary study,[39] application of 2D [^{15}N,^{1}H]-TROSY-H(N)N-COSY revealed the presence of $^{h2}J_{N,N}$ interactions between FMN N(1) and the amide nitrogen of Asp95 in both redox states. However, quantification was complicated by partial overlap of the Asp95 diagonal peak in the oxidized state, and additional interactions might have been masked by adjacent strong diagonal peaks. The experiments were therefore repeated in a 3D version, modified as described in the Experimental Section.

The relevant nitrogen–nitrogen correlations observed for oxidized and fully reduced flavodoxin are compared in Figure 2. The above-mentioned Asp95 N′–FMN N(1) hydrogen bridge manifests itself as a cross-peak at the ^{15}N chemical shift of the FMN N(1) acceptor nitrogen (oxidized state: $\delta =$ 186.4 ppm; reduced state: $\delta = 185.0$ ppm) along the F_1 dimen-

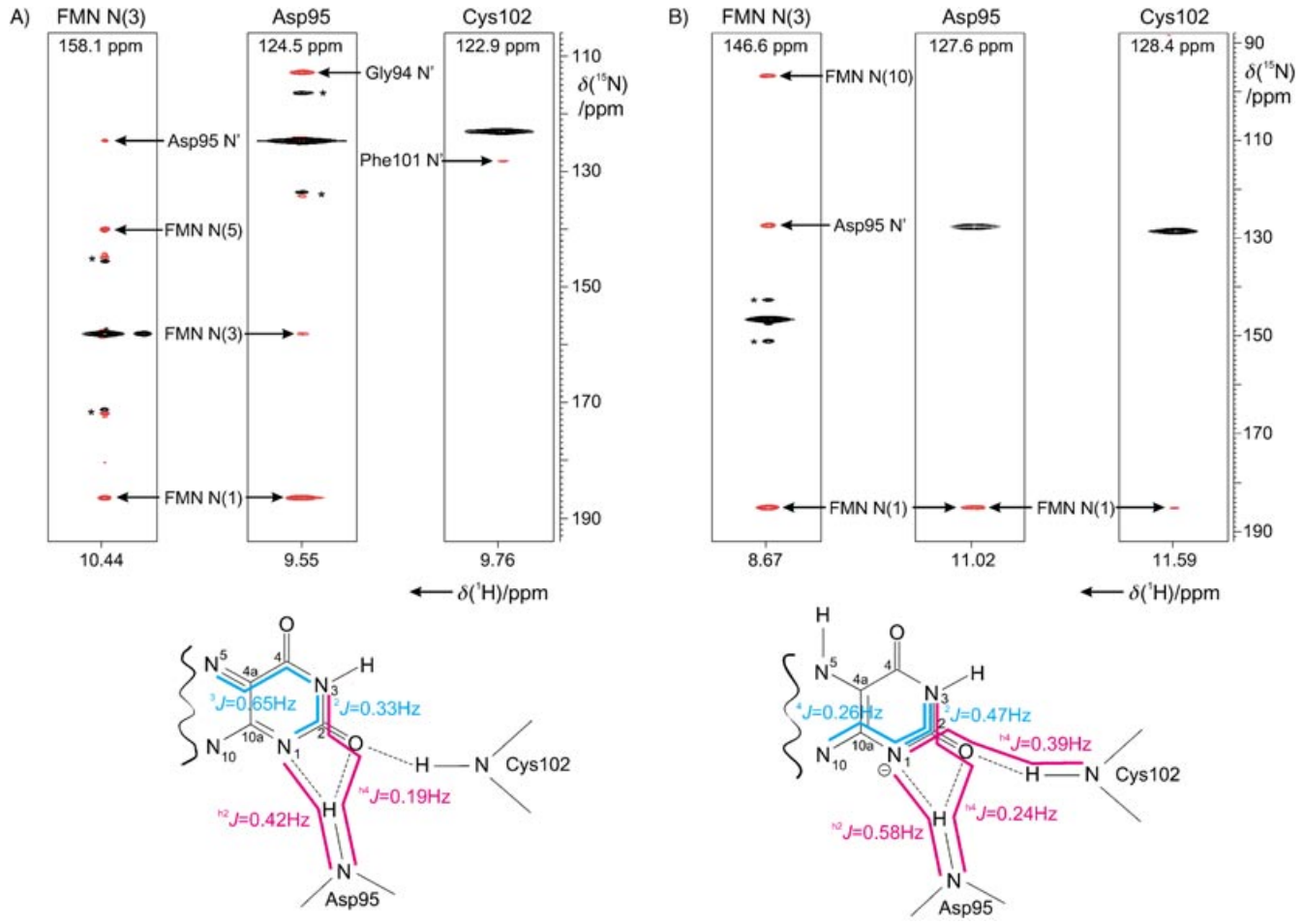

Figure 2. *Scalar ^{15}N–^{15}N correlations in A) oxidized and B) fully reduced* D. vulgaris *flavodoxin. Top:* F_1 *(^{15}N)-F_3 (^{1}H) strips (widths: 0.24 ppm) from 3D [^{15}N,^{1}H]-TROSY-HNN-COSY spectra taken at the F_2 (^{15}N) positions of FMN N(3), Asp95 N′, and Cys102 N′ and centered at the F_3 (^{1}H) chemical shifts given at the bottom of each panel. Positive (diagonal peaks) and negative (cross-peaks) intensities are represented by black and red contours, respectively. The FMN N(5) resonance of oxidized flavodoxin is aliased in the F_1 dimension and corresponds to a chemical shift of 338 ppm. Artifact peaks appearing symmetrically with respect to very strong diagonal peaks along F_1 are indicated with asterisks. Bottom: scheme showing the observed scalar connectivities involving FMN nitrogens and the corresponding coupling constants as determined from cross-peak/diagonal peak intensity ratios. Regular J couplings and trans-H-bond (^{h}J) couplings are indicated in cyan and magenta, respectively.*

 © 2004 Wiley-VCH Verlag GmbH & Co. KGaA, Weinheim

sion at the $^{15}N/^{1}H$ (F_2/F_3) positions of the donor amide group. Owing to the dispersion along the third dimension the Asp95 diagonal signal is now completely resolved, allowing the determination of the corresponding $^{h2}J_{N,N}$ coupling constants, which amount to 0.42 Hz in the oxidized state and 0.58 Hz in the reduced state. In addition, a weak $^{h4}J_{N,N}$ interaction between Asp95 N′ and FMN N(3) is established by a pair of cross-peaks at the $^{15}N/^{1}H$ (F_2/F_3) positions of both NH groups in the oxidized state. The same correlation is also observed in the reduced state, although it could only be detected in the FMN N(3) slice. On the other hand, $^{h4}J_{N,N}$ coupling between Cys102 N′ and FMN N(1) exists exclusively in the reduced state. Notably, both types of $^{h4}J_{N,N}$ interaction had formerly escaped detection when the 2D [^{15}N,^{1}H]-TROSY-H(N)N-COSY version was applied.[39]

At first sight, the lower cross-peak intensities observed in the reduced state appear to be inconsistent with higher magnitudes of the associated *J* couplings when compared to the oxidized state. This can, however, be attributed to the generally lower sensitivity of all experiments carried out on reduced flavodoxin, for reasons discussed below. The relative sensitivity of spectra recorded in the two states can be gauged from vicinal ^{15}N–^{15}N couplings in the protein backbone, which are readily observed in the oxidized state ($^{3}J_{Asp95\,N',Gly94\,N'} = 0.30$ Hz; $^{3}J_{Cys102\,N',Phe101\,N'} = 0.26$ Hz),[40] whereas they did not give rise to cross-peaks in the reduced state. To the best of our knowledge, four-bond nitrogen–nitrogen coupling across H-bonds has so far been reported only for a G·G·G·G tetrad in a DNA quadruplex,[23] in which it was found to be slightly smaller than the values measured in flavodoxin. It should be noted that there are two possible pathways for the $^{h4}J_{Asp95\,N',FMN\,N(3)}$ interaction since the Asp95 amide forms a bifurcated H-bond with N(1) and O(2) as acceptors.[3b,f] Experimentally it cannot be distinguished which of these branches contributes to the observed scalar coupling or whether it is a combination of both.

Long-range ^{15}N,^{15}N *J* couplings within the flavin ring system are also detected in the [^{15}N,^{1}H]-TROSY-HNN-COSY spectra. The two-bond $^{15}N(3)$,$^{15}N(1)$ interaction is observed in both redox states and is found to be somewhat larger in the reduced flavin. In contrast, a relatively large ^{3}J coupling between N(3) and N(5) appears to exist exclusively in the oxidized state. It should be mentioned that, while this correlation is detected in the [^{15}N,^{1}H]-TROSY-HNN-COSY spectrum of Figure 2A despite the large offset of the $^{15}N(5)$ resonance ($\delta = 338$ ppm), its magnitude would be severely underestimated because of the finite excitation bandwidth of the ^{15}N radio frequency pulses. Instead, the value reported in Figure 2 was measured accurately by using a pseudo-heteronuclear variant of the experiment[41] (not shown), in which pulses on resonance with the two ^{15}N nuclei are applied sequentially. A weak four-bond coupling between N(3) and N(10) was detected in the reduced but not in the oxidized state. Again, two pathways (i.e., via C(4) and C(4a) or via C(2) and N(1)), are conceivable. Although they cannot be distinguished experimentally it is likely that the latter makes a larger contribution since the $^{3}J_{N(3),N(5)}$ coupling, which shares two bonds with the N(3)-C(4)-C(4a)-C(10a)-N(10) pathway, is vanishingly small in reduced flavodoxin. While it is not unexpected that the homonuclear scalar interactions of the nitrogen nuclei in the flavin differ between the two redox states as a consequence of pronounced changes in electron densities, to the best of our knowledge, this study has experimentally demonstrated this effect in a flavoprotein for the first time.

Measurement of $^{h}J_{C,N}$ coupling constants

Three-bond $^{13}C'$,^{15}N couplings across N–H···O=C H-bonds in proteins are commonly probed by long-range HNCO-type experiments.[19,20,42,43] Unlike their homonuclear counterparts, such *J*-correlated spectra do not contain diagonal peaks that could be exploited to determine coupling constants from intensity ratios. Quantification therefore usually involves recording of separate reference spectra containing sequential cross-peaks due to magnetization transfer through $^{1}J_{C',N}$ couplings. A different strategy was followed in the current study. Intermolecular $^{h3}J_{C,N}$ coupling constants were measured by use of 3D quantitative *J*-correlated [^{15}N,^{1}H]-TROSY-HNC pulse sequences that give rise to internal reference signals.[44] This approach is less susceptible to peak-integration errors in separate spectra, possibly of different dimensionality, nonuniform $^{1}J_{C',N}$ reference coupling constants, and sample instability. The last point was of particular relevance for reduced flavodoxin samples, which showed signs of partial reoxidation after approximately two days in the spectrometer.

The method is outlined in Figure 3. Briefly, following the initial INEPT[48] sequence, magnetization is transferred from nitrogens to scalar coupled carbon spins in an HMQC manner,[49] upon which ^{13}C magnetization is frequency-labeled during t_1. Quadrature in the F_1 dimension is achieved by a modified STATES[47] scheme by use of an $x/-x$ phase cycling of the ^{13}C 90° pulse following t_1 in concert with the receiver reference phase in the imaginary part but not in the real part of each t_1 increment. As a result, magnetization components not transferred from ^{15}N to ^{13}C during the Δ periods are cancelled in the imaginary part of the t_1 interferogram while being retained in the real part. As schematically shown at the bottom left of Figure 3, this gives rise to a signal devoid of chemical shift modulation but subject to ^{15}N transverse relaxation, superimposed on the components that were transferred by ^{15}N,^{13}C scalar interactions. The latter evolve as multiple quantum coherences carrying ^{13}C chemical shift information. After Fourier transformation, spectra therefore contain cross-peaks at the ^{13}C pseudo-single quantum positions along F_1 as well as an axial peak (i.e., at zero frequency), which takes the role of diagonal peaks in homonuclear quantitative *J* correlations, thus enabling the measurement of coupling constants from intensity ratios.

The basic [^{15}N,^{1}H]-TROSY-HNC pulse sequence shown in Figure 3 was applied to oxidized flavodoxin in order to investigate a potential H-bond of the FMN N(3)H group. A common difficulty in heteronuclear quantitative *J*-correlation experiments is the suppression of magnetization transfer through large one-bond couplings that would otherwise completely degrade the efficiency of the transfer via the much smaller scalar interactions to be studied. This can be achieved by setting the transfer period Δ to a multiple of the inverse of the ^{1}J coupling

 © 2004 Wiley-VCH Verlag GmbH & Co. KGaA, Weinheim

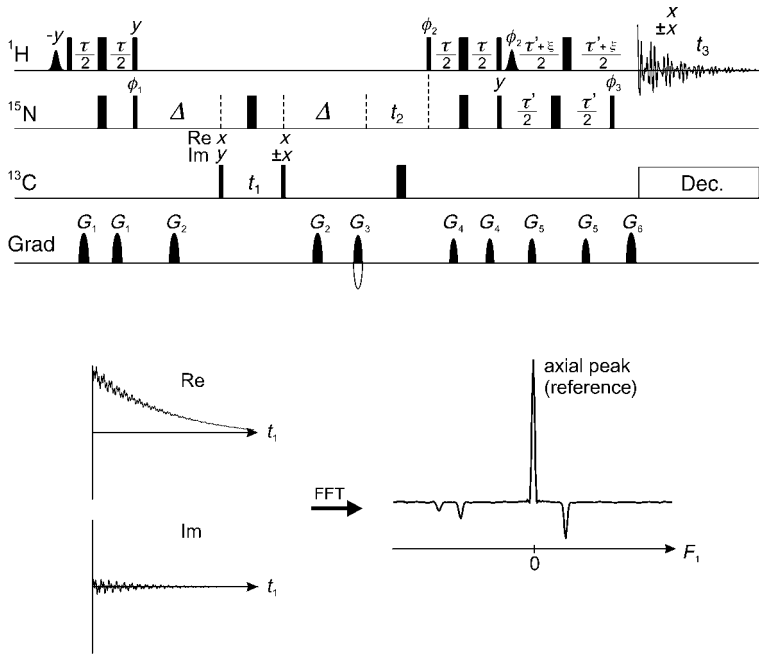

Figure 3. *Top: Generic [^{15}N,^{1}H]-TROSY-HNC quantitative J-correlation pulse scheme, as employed to determine ^{15}N,^{13}C coupling constants involving N(3) of FMN in oxidized flavodoxin. Narrow and wide bars denote rectangular 90° and 180° pulses, respectively, applied with RF fields (at carrier positions) of 19.4 kHz (7.8 ppm) for ^{1}H, 6.9 kHz (157 ppm) for ^{15}N, and 16.7 kHz (148.4 ppm) for ^{13}C. Selective ^{1}H water flip-back pulses[45] have a Gaussian shape, truncated at 10%, and a duration of 2 ms. Optional heteronuclear decoupling during acquisition to eliminate unresolved long-range $^1H^{N(3)}$,^{13}C couplings employs a 1.7 kHz GARP-1[46] modulation. The period Δ is adjusted as described in the text. Delays τ, τ', and ξ have durations of 4.6, 5.4, and 0.4 ms, respectively. Sine-bell shaped z-gradient pulses have the following lengths and peak amplitudes: G_1, 0.5 ms, 5 G cm^{-1}; G_2, 0.5 ms, 7.5 G cm^{-1}; G_3, 1.6 ms, 19.73 G cm^{-1}; G_4, 0.3 ms, 4 G cm^{-1}; G_5, 0.3 ms, 5.5 G cm^{-1}; G_6, 0.2 ms, 16 G cm^{-1}. Pulse phases are x unless otherwise stated. Phase ϕ_1 is cycled x,−x along with the receiver, ϕ_2=y, ϕ_3=x. Echo and anti-echo coherence transfer pathways are selected alternately by inverting the polarity of G_3 and pulse phases ϕ_2 and ϕ_3. Quadrature detection in F_1 is achieved by the STATES[47] protocol by using different phase cycles for the real and imaginary parts as explained in the text. Bottom: schematic representation of the real and imaginary parts of a resulting t_1 interferogram and the corresponding F_1 cross section after complex Fourier transformation.*

constant. In the long-range HNCO experiment described above this is relatively straightforward, because there is only a single $^1J_{C',N}$ coupling, which has a well known range in protein backbones. In contrast, the isoalloxazine ring has a more complex spin topology. Therefore, in a first step, the quantitative *J*-correlated [^{15}N,^{1}H]-TROSY-HNC experiment was carried out with a short Δ delay (15 ms) to determine the coupling constants between the N(3) nucleus and its adjacent ring carbons. The leftmost strip in Figure 4A represents an expansion from the resulting spectrum, showing three cross-peaks at the chemical shifts of the FMN ^{13}C(2), ^{13}C(4), and ^{13}C(4a) nuclei. Evaluation of cross-peak/axial peak intensity ratios yielded coupling constants of 11.6, 12.9, and 6.5 Hz for $^1J_{C(2),N(3)}$, $^1J_{C(4),N(3)}$, and $^2J_{C(4a),N(3)}$, respectively. The one-bond coupling constants are in good agreement with values obtained for free flavins by 1D direct observation ^{15}N and ^{13}C spectroscopy,[15a,50] whereas the two-bond coupling is considerably stronger than determined previously,[15a] where the limited sensitivity and resolution of the 1D ^{15}N spectra might have impeded its accurate determination in the presence of additional ^1J splittings. The experiment was then repeated with a Δ value adjusted to 162.5 ms$\approx 2/^1J_{C(2),N(3)} \approx 2/^1J_{C(4),N(3)} \approx 1/^2J_{C(4a),N(3)}$ to minimize the magnetization transfer along these pathways. As a result, the one-bond and two-bond correlations are still observed due to an unavoidable Δ mismatch (Figure 4A, second strip from left), but the presence of these large couplings was no longer prohibitive for transfer of magnetization through ^{13}C,^{15}N *J* interactions that are at least an order of magnitude smaller. This enabled the detection of a cross-peak at the position of the Tyr100 carbonyl resonance (δ= 178.2 ppm), providing evidence for an intermolecular H-bond. By using the axial peak as internal reference the cross-peak intensity translates into a $^{h3}J_{Tyr100C',FMN N(3)}$ coupling constant of 0.26 Hz. Additional cross-peaks arise through long-range correlations within the isoalloxazine ring system (i.e., $^3J_{C(10a),N(3)}$= 0.91 Hz and $^4J_{C(5a),N(3)}$=0.30 Hz.

Attempts to observe an analogous trans-H-bond scalar coupling in the reduced state failed. Measurements of one-bond and two-bond couplings revealed an increase in $^1J_{C(2),N(3)}$ (13.0 Hz) and a decrease in $^2J_{C(4a),N(3)}$ (5.0 Hz), rendering simultaneous matching of Δ to the inverse of all three *J* values impossible. However, since the ^{13}C(4a) resonance in reduced flavodoxin is shifted upfield to approximately 104 ppm,[15b] the two-bond coupling can be selectively refocused, allowing Δ to be adjusted to 153 ms$\approx 2/^1J_{C(2),N(3)} \approx 2/^1J_{C(4),N(3)}$. At the ^{15}N/^{1}H ($F_2/F_3$) position of FMN N(3)H, the corresponding spectrum exclusively contained cross-peaks due to the residual $^1J_{C(2),N(3)}$ and $^1J_{C(4),N(3)}$ couplings (Figure 4B). The absence of a cross-peak at the Tyr100 ^{13}C′ chemical shift (δ=177.3 ppm) does not completely rule out the existence of a H-bond, but an upper limit of 0.17 Hz can be calculated for $^{h3}J_{Tyr100C',FMN N(3)}$ in the reduced state from the noise amplitude and the intensity of the axial peak. The same holds for regular long-range $J_{C,N(3)}$ couplings that were likewise not observable.

Reduction of the flavin is followed by protonation of the N(5) nitrogen, introducing a second potential H-bond donor. In fact, X-ray structure analysis[3f] has revealed a conformational rearrangement of the protein backbone in *D. vulgaris* flavodoxin, resulting in the formation of an intermolecular N(5)–H···O= C(Gly61) hydrogen bridge in the reduced state (Figure 1). The major obstacle for NMR investigation of this interaction is the near degeneracy of the N(5)H proton resonance (δ=4.84 ppm) with the water signal. This rather unusual $^1H^N$ chemical shift is in reasonable agreement with a previously reported assignment (δ=5.13 ppm at *T*=303 K and pH 8.3).[34c] In contrast, at pH 7 the ^{1}H(5) resonance is not observable at temperatures above 295 K and below this temperature has chemical shifts around 7.0 ppm.[51] To increase the separation by approximately 0.1 ppm (at 900 MHz; $^1J_{N(5),H}$=86.4 Hz) the [^{15}N,^{1}H]-"TROSY"-HNC experiment involved recording of the "south-west" semi-TROSY ^{1}H,^{15}N 2D doublet component at the cost of a minor line-broadening in the ^{1}H dimension, while the more slowly

 © 2004 Wiley-VCH Verlag GmbH & Co. KGaA, Weinheim

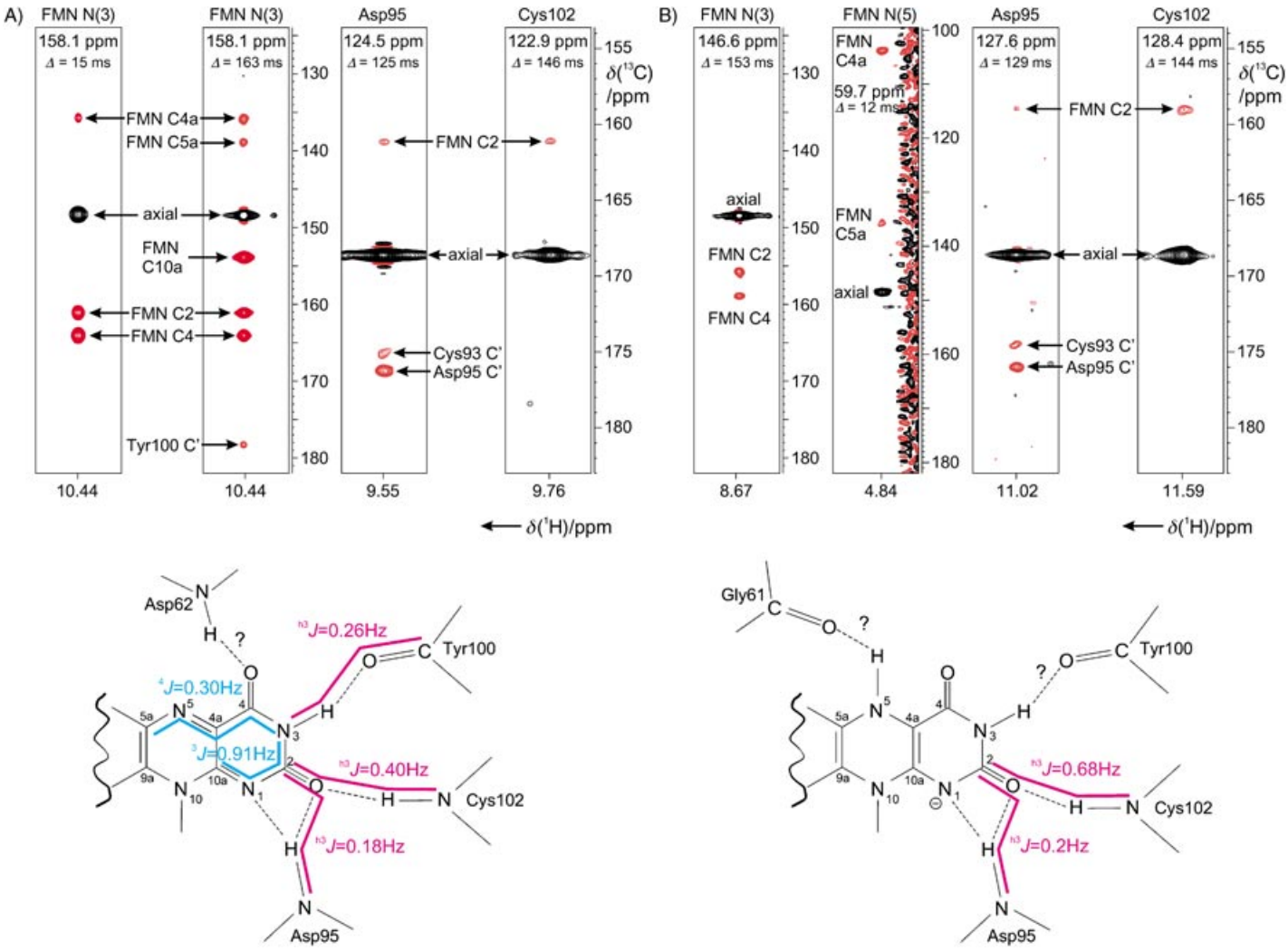

Figure 4. *Multiple-bond $^{13}C,^{15}N$ couplings in A) oxidized, and B) fully reduced* D. vulgaris *flavodoxin as determined by internally referenced quantitative* J *correlation. All strips have a width of 0.24 ppm along the F_3 (^1H) dimension and are centered at the chemical shifts indicated at the bottom. Positions in the F_2 (^{15}N) dimension are given at the top of each strip, along with the value of the $^{15}N,^{13}C$ transfer time Δ employed in the individual [$^{15}N,^1H$]-TROSY-HNC experiments. Positive and negative intensities are represented by black and red contours, respectively. The resulting values of trans-H-bond (^{h}J, magenta) and intramolecular long-range (J, cyan) coupling constants are given in the lower part of the figure.*

decaying ^{15}N component was still selected during the Δ and t_2 periods. This modification allowed the observation of one-bond correlations (Figure 4B, second strip from left) when $\Delta =$ 12 ms was chosen, yielding 14.4 and 11.7 Hz for $^1J_{C(4a),N(5)}$ and $^1J_{C(5a),N(5)}$, respectively. Adjustment of Δ to significantly longer values in order to probe a potential $^{h3}J_{Gly61\,C',FMN\,N(5)}$ coupling resulted in a complete loss of signal. It cannot be excluded that the reduced flavodoxin samples employed here contained trace amounts of semiquinone, entailing accelerated relaxation of ^{15}N and ^1H magnetizations at the N(5) position due to fast electron exchange between fully reduced and semiquinone species. Furthermore, the sensitivity of all proton–nitrogen correlation experiments directed towards the detection of the N(5)H resonance was reduced because the water flip-back[45] procedure could not be applied.

Significantly improved efficiency of through-hydrogen bond $^{15}N,^{13}C$ correlations of main-chain amide nitrogens in non-deuterated proteins can be achieved by composite pulse decoupling of α-carbons,[52] which suppresses scalar relaxation of the second kind.[53] Consequently, quantitative *J*-correlated [$^{15}N,^1H$]-TROSY-HNC experiments directed towards the identification of intermolecular H-bond donors of apoflavodoxin included band-selective $^{13}C^\alpha$ decoupling during the Δ periods resulting in sensitivity enhancements of between 20 and 25%. Measurements involving the Asp95 amide required additional refocusing of the relatively large intraresidual $^3J_{N',C_\gamma}$ coupling amounting to 2.25 Hz.[54] Separate experiments were performed for individual amides in order to adjust Δ to $2/^1J_{C',N}$ according to previously determined one-bond coupling constants.[44c] For details regarding all modifications of the basic pulse scheme of Figure 3 in the various [$^{15}N,^1H$]-TROSY-HNC quantitative *J*-correlation experiments, see the Experimental Section.

Both the Asp95 NH and the Cys102 NH of oxidized flavodoxin are hydrogen-bonded to FMN O(2), as attested by $^{h3}J_{C,N}$ correlations in [$^{15}N,^1H$]-TROSY-HNC spectra (Figure 4A). Although the cross-peaks are of similar intensity, the $^{h3}J_{FMN\,C2,Cys102\,N'}$ cou-

 © 2004 Wiley-VCH Verlag GmbH & Co. KGaA, Weinheim

pling constant is found to be larger as becomes apparent by reference to the respective axial peaks. The reasons for the reduced overall intensity in the Cys102 strip are the faster transverse relaxation of its amide nuclei and the longer Δ period used. Of the two cross-peaks in the low-field half of the Asp95 strip, the one at 176.3 ppm is due to the intraresidual two-bond coupling ($^2J_{C',N} = 0.35$ Hz) while the second exactly matches the Cys93 $^{13}C'$ chemical shift[55] such that it is tentatively assigned to a four-bond interaction ($^4J_{Cys93\,C',Asp95\,N'} = 0.23$ Hz) along the protein main chain. In contrast, the large sequential and intraresidual correlations with Gly94 C′ ($\delta = 173.7$ ppm) and Asp95 C^{γ} ($\delta = 179.9$ ppm), respectively, have been effectively suppressed. No indication for the putative H-bond between the Asp62 amide and FMN O(4) could be obtained from quantitative *J*-correlation experiments (not shown). The reference peak intensity determines an upper limit of 0.23 Hz for the $^{h3}J_{FMN\,C(4),Asp62\,N'}$ coupling constant. The fact that transverse ^{15}N magnetization of Asp62 decays more rapidly than that of most other amides in flavodoxin[56] explains why this value is higher than the one that could be readily measured for the FMN C(2),Asp95 N′ interaction.

By similar methodology, Asp95/Cys102 to FMN O(2) H-bonds were also directly observed through scalar couplings in the reduced state (Figure 4B). While the magnitude of $^{h3}J_{FMN\,C(2),Asp95\,N'}$ lies in the same range for both redox states, $^{h3}J_{FMN\,C(2),Cys102\,N'}$ is significantly larger in reduced flavodoxin. Again, the overall signal-to-noise ratio in the spectra of the latter species is apparently lower, which is a consequence of: 1) lower protein concentrations, 2) higher buffer concentrations, 3) enhanced solvent exchange due to higher pH values, and 4) the usually shorter measurement times imposed by its limited stability. It is therefore to be expected that the values reported for the hydroquinone species should be somewhat less precise than those for the oxidized form. It should be mentioned here that all quantitative *J*-correlation experiments of oxidized flavodoxin were performed in triplicate in order to assess their precision. This was made possible by the high stability of this redox state. In no case did the variations of measured coupling constants exceed 0.04 Hz, indicating that—despite their very low magnitudes—reliable values were being obtained.

Measurements of $^hJ_{H,N}$ and $^hJ_{H,C}$ coupling constants in oxidized flavodoxin

Besides through-bond interactions between heteronuclei on both sides of a H-bond, *J* couplings were detected between the bridging hydrogen nuclei and the acceptor group heteronuclei.[18,21,24,25] E.COSY-type[57] methods for the determination of $^{h1}J_{H,N}$ rely on relatively large $^{h2}J_{N,N}$ interactions either to separate doublet components corresponding to the two spin states of a passive ^{15}N nucleus along an orthogonal dimension[58] or to transfer magnetization to the acceptor nitrogen in order to measure the ^{15}N frequency difference in two subspectra representing the donor ^1H α and β spin states.[18] As the $^{h2}J_{N,N}$ couplings observed in flavodoxin are far too small to give rise to splittings, the second option, a ^1H spin-state-selective (S^3) 2D [^{15}N,^1H]-TROSY-H(N)N experiment, was chosen here. Because of the long $^{h2}J_{N,N}$ transfer time required, it was essential to use a version of the pulse sequence that selects for the TROSY component during both Δ periods and either leaves ^1H spin states unperturbed or inverts them immediately before and after the t_1 evolution time[59,60] (for details see the Experimental Section).

The $^{15}N(1)$-{^1H} doublet components of the Asp95 H^N–FMN N(1) cross-peak taken from the two ^1H–S^3 [^{15}N,^1H]-TROSY-H(N)N subspectra of oxidized flavodoxin are shown in Figure 5A–C. They exhibit a very small, yet measurable displacement of 0.25 Hz along the ^{15}N dimension, corresponding to the intermolecular $^{h1}J_{Asp95\,HN,FMN\,N(1)}$ coupling. Repeating the experiment three times indicated an uncertainty of less than ± 0.1 Hz. The

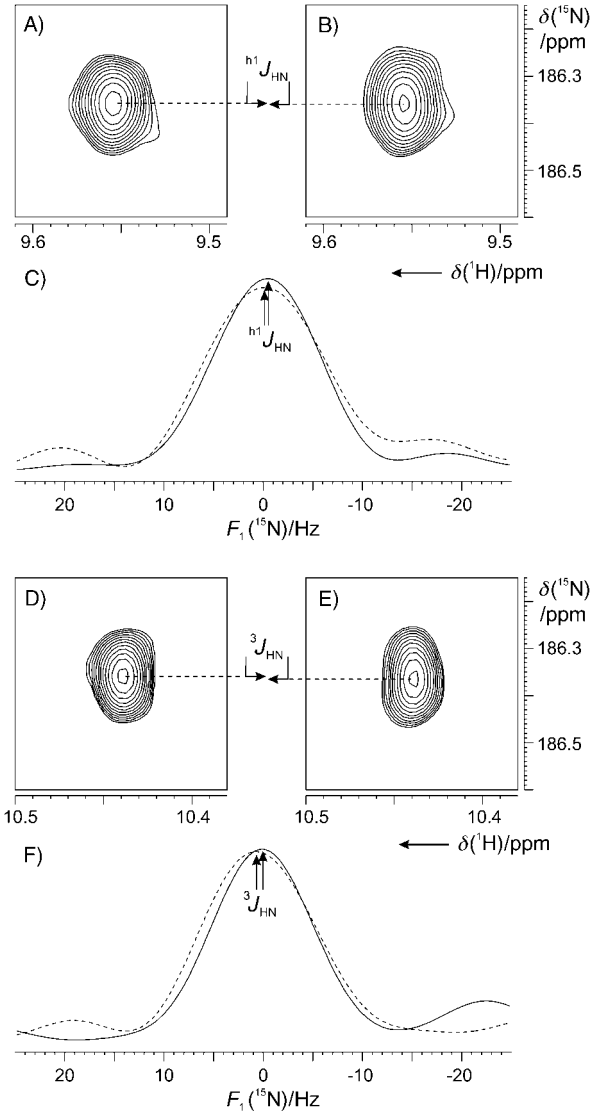

Figure 5. *Determination of A)–C) $^{h1}J_{Asp95\,HN,FMN\,N(1)}$ and D)–F) $^3J_{FMN\,H(3),N(1)}$ in oxidized flavodoxin. Contour plots A), D), and B), E) are taken from subspectra of the 2D ^1H-S^3 [^{15}N,^1H]-TROSY-H(N)N experiment with selection of the $^1H^N$ β (no 180° pulses before and after t_1) and α spin states, respectively. Traces along the F_1 (^{15}N) dimension taken from A), B), and from D), E) are superimposed in C) and F), respectively, where the solid line represent the $^1H^N$ β and the dashed line the α spin state. The horizontal displacement between the two ^{15}N-{^1H} doublet components corresponds to the C) ^{h1}J and F) ^3J coupling constants as indicated.*

 © 2004 Wiley-VCH Verlag GmbH & Co. KGaA, Weinheim

sign of the coupling is opposite to that of the $^{1}J_{H,N}$ coupling of the Asp95 autocorrelation peak (i.e., positive). This is consistent with results obtained for nucleic acid-base pairs, where $^{h1}J_{H,N}$ couplings were found to be positive and of approximately half the size of the associated $^{h2}J_{N,N}$ interaction.[18,21,59–61] The extraction of the three-bond coupling between FMN N(1) and the H(3) from the intramolecular $^{15}N(3),^{15}N(1)$ correlation in the same spectrum is shown in Figure 5 D–F. It is also positive and has a value of 0.6 Hz, which is similar in magnitude to the $^{3}J_{H(3),N(1)}$ coupling (0.9 Hz) reported for oxidized riboflavin tetrabutyrate dissolved in chloroform.[50] Analogous experiments directed towards the measurement of $^{h2}J_{FMN\,H(3),Tyr100\,C'}$ and $^{h2}J_{Cys102\,HN,FMN\,C(2)}$ employed a ^{1}H-S^{3} [^{15}N,^{1}H]-TROSY-H(N)C pulse sequence[25] with Tyr100 $^{13}C'$ and FMN $^{13}C(2)$ selective pulses, respectively, and yielded coupling constants between 0 and 1 Hz (results not shown). Unfortunately, the variations upon repeated measurements were of the same order of magnitude, indicating that the sensitivity was not sufficient to provide reliable results. Since information from $^{h1}J_{H,N}$ and $^{h2}J_{H,C}$ coupling constants is to some extent redundant to that available from $^{h2}J_{N,N}$ and $^{h3}J_{C,N}$, respectively, and their precision depends strongly on the signal-to-noise ratios that can be obtained, these experiments were not attempted for reduced flavodoxin.

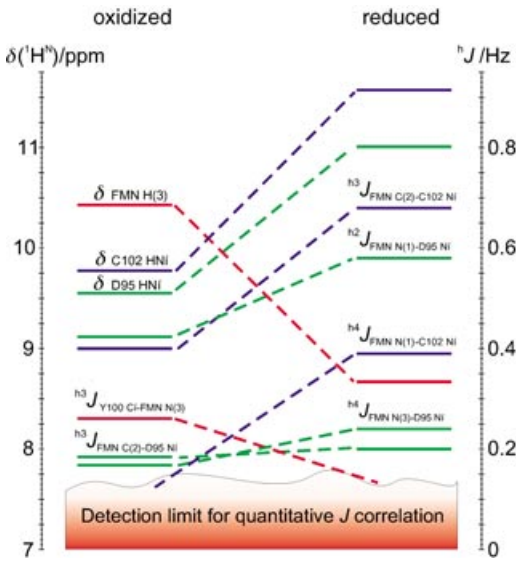

Figure 6. *Comparison of ^{h}J coupling constants and $^{1}H^{N}$ chemical shifts in oxidized (left) and fully reduced (right) flavodoxin. Vertical scales on the left-hand and right-hand sides apply to chemical shifts and coupling constants, respectively, for both redox states. Experimental data involving FMN N(3)H, Asp95 HN′, and Cys102 HN′ donor groups are represented in red, green, and blue, respectively. The lower limit for $^{h}J_{N,N}$ and $^{h}J_{C,N}$ couplings to give rise to detectable cross-peaks in quantitative J correlation experiments ("detection limit") depends on the reference peak intensity and the noise level in the individual spectra and was found to vary between 0.13 and 0.18 Hz. No information was obtained for putative through-hydrogen-bond scalar couplings between Asp62 $^{15}N'$ and FMN $^{13}C(4)$ in the oxidized state and between Gly61 $^{13}C'$ and FMN $^{15}N(5)$ in the reduced state, where the experimental sensitivity was considerably lower.*

Correlations with chemical shifts and H-bond lengths

For both proteins[19] and nucleic acids[21] clear correlations of the isotropic chemical shifts of the H-bonded proton and ^{h}J coupling constants have been observed. An H···O distance dependence of $\delta_{H,N}$ in proteins has long been recognized,[15,16,62] with short H-bond lengths corresponding to larger values for the chemical shift. Although density functional theory calculations indicate that angular dependencies cannot be neglected,[63] trans-H-bond scalar couplings are predominantly determined by donor–acceptor distances and an exponential relationship between $^{h3}J_{C',N}$ and the N···O distance [$(^{h3}J_{C',N} = -5.9 \times 10^{4}\ \mathrm{Hz} \times \exp[-4 \times R_{NO}\,\text{Å}^{-1}])$] in proteins has been established empirically.[42] Nitrogen–nitrogen and carbon–nitrogen ^{h}J coupling constants measured for flavodoxin in both redox states are summarized in Figure 6 along with the donor $^{1}H^{N}$ chemical shifts. The correlation between the two parameters is obvious. Downfield shifts of the amide proton resonances of Asp95 and Cys102 by 1.47 and 1.83 ppm, respectively, upon two-electron reduction are accompanied by increases in the $^{h2}J_{FMN\,N(1),Asp95\,N'}$ and $^{h3}J_{FMN\,C(2),Cys102\,N'}$ coupling constants. In the same sense, $^{h3}J_{FMN\,C(2),Asp95\,N'}$ and $^{h4}J_{FMN\,N(3),Asp95\,N'}$ become slightly larger and the $^{h4}J_{FMN\,N(1),Cys102\,N'}$ interaction is exclusively observed in the reduced state. Conversely, $^{h3}J_{Tyr100\,C',FMN\,N(3)}$ coupling is only detectable in the oxidized state, where the chemical shift of the proton within the H-bond is 1.77 ppm downfield from that in the reduced state.

Qualitatively, these results are in accordance with donor–acceptor distances measured in low-temperature crystal structures of oxidized and fully reduced flavodoxin[3f] (Figure 1); that is, the Asp95 N′···N(1) and Cys102 N′···O(2) distances become shorter when flavodoxin is reduced. Interestingly, a somewhat larger Asp95 N′···N(1) distance was observed in a more recent 2.5 Å refined X-ray structure of the oxidized apoflavodoxin–FMN complex[64] and since, additionally, the Asp95 N–H···N(1) bond angle (122.5°) deviates considerably from optimal geometry it has been considered unlikely that this H-bond actually occurs.[65] This conclusion appears to be in contradiction with our results. However, it should be noted that the $^{h2}J_{FMN\,N(1),Asp95\,N'}$ coupling constants are about one order of magnitude smaller than $^{h2}J_{N,N}$ values measured in nucleic acid-base pairs[17,18,21,41,66] and between imidazole nitrogens of two histidine residues in a protein,[67] suggesting that the Asp95 N–H···N(1) H-bond is weak but not absent in solution. Furthermore it cannot be ruled out that the detected "$^{h2}J_{N,N}$" couplings include a contribution from a second pathway via the Asp95 N–H···O=C(2) H-bond and the coupling constants are the composite of two-bond and four-bond scalar interactions across two distinct H-bonds.

In reduced FMN the negative charge of the anionic isoalloxazine ring was found to be located at the N(1)–C=O(2) moiety.[15] When bound to apoflavodoxin, strengthening of intermolecular H-bonds in this region occurs upon two-electron reduction, as evidenced by increased ^{h}J coupling constants involving the $^{15}N(1)$ and $^{13}C(2)$ nuclei. This may reflect partial charge delocalization through the amide groups of Asp95 and Cys102, as previously suggested on the basis of ^{1}H chemical shifts.[34c]

 © 2004 Wiley-VCH Verlag GmbH & Co. KGaA, Weinheim

Through-hydrogen bond couplings gave little information about the H-bonding pattern of the N(5)–C(4a)–C=O(4) moiety of FMN, information that would be indicative of a conformational change of the apoprotein backbone in response to reduction of the cofactor. While measurement of $^{h3}J_{Gly61\,C',FMN\,N(5)}$ in reduced flavodoxin was impossible for reasons mentioned above, an upper limit can be given for the FMN $^{13}C(4)$–Asp62 $^{15}N'$ scalar coupling in the oxidized species, which precludes a strong H-bond interaction. This is consistent with the comparatively high-field chemical shift ($\delta = 8.78$ ppm) and H/D exchange characteristics of the Asp62 amide proton.[34] Furthermore, structural investigation of oxidized *D. vulgaris* flavodoxin in solution[4e] revealed an even longer donor–acceptor distance for the putative H-bond than in the crystal structure.

The elongation of the Tyr100 (C′)O–FMN N(3) distance by 0.23 Å observed in the X-ray structures is reflected by the fact that a $^{h3}J_{Tyr100\,C',FMN\,N(3)}$ coupling constant of 0.26 Hz is measured in the oxidized state, whereas it is below the detection limit (0.17 Hz) in the reduced state, which may be indicative of a complete breakdown of the N(3)H hydrogen bond. Computational and electrochemical investigations of model systems implied that hydrogen bonding at this position has a marked effect on the redox potential of the flavin system, predicting modulations of up to 80 mV.[68] Systematic replacement of the FMN N(3)H–apoprotein H-bond acceptor in conjunction with ^1H–^{15}N NMR studies on *Clostridium beijerinckii* flavodoxin provided further evidence that this interaction contributes to cofactor binding primarily in the oxidized state and is least important for the fully reduced state.[69]

In conclusion, we have demonstrated that the measurement of ^hJ couplings is suitable for the identification of intermolecular H-bond interactions in protein–cofactor complexes. Though small, their magnitudes can be determined precisely by the use of TROSY-based[70] quantitative *J*-correlation experiments in conjunction with high polarizing fields. Therefore, subtle changes of H-bond strengths upon reduction of the flavin in *D. vulgaris* flavodoxin could be probed through concomitant $^hJ_{N,N}$ and $^hJ_{C,N}$ coupling constants. Differential thermodynamic stabilization of the three accessible redox states of flavodoxin-bound FMN by H-bond interactions is likely to contribute to the observed shifts of midpoint potentials relative to free FMN. The results presented here suggest trans-H-bond scalar couplings as a useful tool with which to investigate correlations between redox potentials and individual intermolecular H-bond strengths in flavoproteins. More generally, owing to the structural similarity between the isoalloxazine ring system and nucleobases, it may be expected that hydrogen bridges at macromolecular interfaces such as protein–nucleic acid complexes might be identified in a similar manner.

Experimental Section

Sample preparation: Recombinant [*U*-^{15}N]- and [*U*-^{13}C,^{15}N]-labeled *D. vulgaris* flavodoxin was expressed in *Escherichia coli* TG1 and grown on M9 medium containing [^{15}N]ammonium chloride (1 g L^{-1-1}) as the sole nitrogen source and either unlabeled or [$^{13}C_6$]glucose (2 g L^{-1}) as well as unlabeled or [$^{13}C_3$]glycerol as carbon sources. Protein expression was induced by the addition of isopropyl β-D-thiogalactopyranoside (IPTG; 20 μM) when the cells reached an $O.D._{600}$ between 0.4 and 0.5. The protocol for purification has been described elsewhere.[34a,36] Oxidized flavodoxin was dissolved in potassium phosphate buffer (pH 7.0, 20 mM) at concentrations of 4.5 mM and 2.1 mM for ^{15}N- and $^{13}C/^{15}N$-labeled protein, respectively. Samples were placed in Shigemi microcells with total volumes of 300 μL. To obtain the hydroquinone redox state, flavodoxin solutions (500 μL, 4.0 mM ^{15}N-labeled and 1.5 mM $^{13}C/^{15}N$-labeled) containing sodium pyrophosphate (pH 8.5, 100 mM) were made anaerobic by successive cycles of degassing and flushing with oxygen-free argon. NMR tubes sealed with serum caps were connected to a vacuum line through syringe needles. A threefold molar excess of anaerobic sodium dithionite solution prepared in the same buffer was added by gas-tight Hamilton syringe. All samples contained D_2O (5%), sodium azide (0.02%), Pefabloc protease inhibitor (50 μg mL^{-1}), EDTA (0.3 mM), and 4,4-dimethyl-4-silapentane-1-sulfonate (DSS; 0.15 mM).

NMR spectroscopy: All pulse sequences applied in this study were of the TROSY[70] type and employed a gradient echo/anti-echo coherence selected, sensitivity-enhanced detection scheme.[71] Experiments were performed at sample temperatures of 300 K on Bruker Avance spectrometers operating at ^1H Larmor frequencies of 800.13 or 900.13 MHz. Quantitative *J*-correlation experiments employed conventional 5 mm single-axis (at 800 MHz) or three-axis gradient (at 900 MHz) $^1H\{^{13}C,^{15}N\}$-triple resonance probes. E.COSY-type $^hJ_{H,N}$ and $^hJ_{H,C}$ measurements were carried out at 900 MHz by use of a cryogenic z-gradient $^1H\{^{13}C,^{15}N\}$-triple resonance probe. Proton chemical shifts were referenced with respect to internal DSS, while indirect calibration of ^{13}C and ^{15}N chemical shift scales employed consensus Ξ ratios.[72]

The HNN-COSY[40] experiment for the measurement of homonuclear ^{15}N,^{15}N couplings was implemented essentially as described by Dingley and Grzesiek.[17] Three modifications are worth mentioning, however: firstly, the rectangular ^{15}N refocusing pulses in the centers of the fixed *J* evolution delays Δ were replaced by pairs of 1.5 ms WURST-20[73] adiabatic pulses (80 kHz sweep), applied at $\Delta/4$ and $3\Delta/4$, to obtain a more uniform transfer efficiency over the widely dispersed ^{15}N chemical shifts of FMN and protein backbone. Secondly, the evolution of $^1J_{N,H}$ couplings in t_1 was refocused by a pair of ^1H 180° pulses.[74] This removes splittings from cross-peaks involving protonated nitrogens while preserving the ^1H spin state corresponding to the slowly relaxing ^{15}N doublet component during both de- and rephasing periods Δ. Thirdly, to reduce signal overlap a third dimension was introduced in a constant-time manner by shifting one of the adiabatic ^{15}N 180° pulses of the second Δ period as a function of t_2.

Heteronuclear ^{13}C,^{15}N coupling constants involving the isoalloxazine $^{15}N(3)$ nucleus of oxidized flavodoxin were measured by the scheme described in Figure 3. To refocus $^2J_{C(4a),N(3)}$ in the reduced species, 2.6 ms G^3 Gaussian cascades,[75] applied at 103.9 ppm, were centered in the two Δ periods. The phase ϕ_3 in the pulse sequence of Figure 3 was inverted to select the low-field ^1H (semi-TROSY) component of the FMN $^1H\{^{15}N(5)\}$ doublet and the ^1H_2O-selective pulses were not applied. For the determination of scalar interactions between amide nitrogens of apoflavodoxin and the isoalloxazine $^{13}C_2$ nucleus in both redox states, the pulse sequence was supplemented with a train of $^{13}C^{\alpha}$-selective adiabatic inversion pulses during the two Δ periods. Pulses were spaced at 2.7 ms and had a WURST-20 shape with a 15 kHz sweep and a duration of 3 ms. When the $^{h3}J_{Asp95\,N',FMN\,C(2)}$ interaction was probed, 2.6 ms G^3 inversion pulses, positioned slightly downfield from the side-chain

 © 2004 Wiley-VCH Verlag GmbH & Co. KGaA, Weinheim

$^{13}CO^{\gamma}$ resonance of Asp95 at 180.6 ppm, were additionally applied in the center of Δ.

Measurements of $J_{N,N}$ in both redox states and of $J_{C,FMN\,N(3)}$ in the oxidized state were performed at 800 MHz, while the remaining experiments were carried out at 900 MHz proton frequency. In all experiments the ^1H carrier was centered in the amide region of the spectrum. Gaussian-shaped water flip-back pulses of 2 ms duration were applied at the H_2O resonance through phase modulation of the radio frequency[76] to avoid saturation of exchanging protons due to gradient dephasing[45] and to achieve effective solvent suppression. The spectral width in the ^1H dimensions was set to 9.0 ppm and the number of data points was adjusted to obtain acquisition times of, typically, 70 ms. The ^{15}N carrier frequency was set at 144 and 137 ppm for [^{15}N,^1H]-TROSY-HNN-COSY experiments on oxidized and reduced flavodoxin, respectively. In [^{15}N,^1H]-TROSY-HNC experiments the ^{15}N carrier was positioned approximately on-resonance with the respective H-bond donor N–H group. Further acquisition parameters and time requirements of the individual quantitative *J* correlations are listed below.

Oxidized flavodoxin: [^{15}N,^1H]-TROSY-HNN-COSY (Δ = 170 ms): spectral widths (SWs) in indirectly detected dimensions $F_1(^{15}N)$ = 99.5 ppm, $F_2(^{15}N)$ = 8.5 ppm, data size 192 (t_1) × 24 (t_2) complex points, acquisition times t_{1max} = 23.7 ms, t_{2max} = 33.6 ms, number of scans per FID (NS) = 8, recording time = 71 h; [^{15}N,^1H]-TROSY-$HN_{FMN\,N(3)}C$ (Δ = 15 ms): SW (F_1, ^{13}C) = 69.0 ppm, SW (F_2, ^{15}N) = 22.0 ppm, 56 (t_1) × 12 (t_2) complex points, t_{1max} = 4.0 ms, t_{2max} = 6.7 ms, NS = 4, recording time = 2.5 h; [^{15}N,^1H]-TROSY-$HN_{FMN\,N(3)}C$ (Δ = 163 ms): SW (F_1, ^{13}C) = 73.1 ppm, SW (F_2, ^{15}N) = 22.0 ppm, 76 (t_1) × 24 (t_2) complex points, t_{1max} = 5.1 ms, t_{2max} = 13.4 ms, NS = 32, recording time = 113 h; [^{15}N,^1H]-TROSY-$HN_{Asp95}C$ (Δ = 125 ms): SW (F_1, ^{13}C) = 30.0 ppm, SW (F_2, ^{15}N) = 7.0 ppm, 66 (t_1) × 36 (t_2) complex points, t_{1max} = 9.7 ms, t_{2max} = 56.4 ms, NS = 16, recording time = 112 h; [^{15}N,^1H]-TROSY-$HN_{Cys102}C$ (Δ = 146 ms): SW (F_1, ^{13}C) = 30.0 ppm, SW (F_2, ^{15}N) = 7.0 ppm, 58 (t_1) × 18 (t_2) complex points, t_{1max} = 8.5 ms, t_{2max} = 28.2 ms, NS = 32, recording time = 90.5 h. Reduced flavodoxin: [^{15}N,^1H]-TROSY-HNN-COSY (Δ = 170 ms): SW (F_1, ^{15}N) = 112.1 ppm, SW (F_2, ^{15}N) = 11.8 ppm, 184 (t_1) × 32 (t_2) complex points, t_{1max} = 20.2 ms, t_{2max} = 33.4 ms, NS = 8, recording time = 90.5 h; [^{15}N,^1H]-TROSY-$HN_{FMN\,N(3)}C$ (Δ = 12 ms): SW (F_1, ^{13}C) = 73.6 ppm, SW (F_2, ^{15}N) = 15.0 ppm, 128 (t_1) × 16 (t_2) complex points, t_{1max} = 7.7 ms, t_{2max} = 11.6 ms, NS = 4, recording time = 15 h; [^{15}N,^1H]-TROSY-$HN_{FMN\,N(3)}C$ (Δ = 153 ms): SW (F_1, ^{13}C) = 66.9 ppm, SW (F_2, ^{15}N) = 15.0 ppm, 112 (t_1) × 20 (t_2) complex points, t_{1max} = 7.4 ms, t_{2max} = 14.6 ms, NS = 16, recording time = 90 h; [^{15}N,^1H]-semi-TROSY-$HN_{FMN\,N(5)}C$ (Δ = 12 ms): SW (F_1, ^{13}C) = 98.2 ppm, SW (F_2, ^{15}N) = 40.0 ppm, 112 (t_1) × 16 (t_2) complex points, t_{1max} = 4.5 ms, t_{2max} = 4.4 ms, NS = 4, recording time = 15 h; [^{15}N,^1H]-TROSY-$HN_{Asp95}C$ (Δ = 129 ms): SW (F_1, ^{13}C) = 32.0 ppm, SW (F_2, ^{15}N) = 20.0 ppm, 80 (t_1) × 12 (t_2) complex points, t_{1max} = 11.0 ms, t_{2max} = 6.6 ms, NS = 32, recording time = 89.5 h; [^{15}N,^1H]-TROSY-$HN_{Cys102}C$ (Δ = 144 ms): SW (F_1, ^{13}C) = 32.0 ppm, SW (F_2, ^{15}N) = 20.0 ppm, 48 (t_1) × 12 (t_2) complex points, $t_{1max} = t_{2max}$ = 6.6 ms, NS = 32, recording time = 48 h.

The determination of one-bond $J_{H,N}$ coupling constants was carried out with a ^1H–S^3 2D [^{15}N,^1H]-TROSY-H(N)N experiment.[59] Modifications of the original pulse sequence included the use of adiabatic ^{15}N 180° pulses during Δ[60] and gradient coherence selection. In addition, the two pairs of ^1H 90° pulses flanking the t_1 evolution time were replaced by $90°_x 180°_\phi 90°_x$ composite pulses, where the phase ϕ was altered between $-x$ and $-y$ to select either TROSY of anti-TROSY components during t_1. The two data sets were recorded in an interleaved manner using $J_{N,N}$ evolution delays (Δ of 120 ms and spectral widths of 127.5 and 15.2 ppm in the ^{15}N (carrier position: 137.1 ppm) and ^1H (carrier position at the ^1H_2O resonance) dimensions, respectively. Time domain data comprised 1396 (t_1) × 1024 (t_2) complex points, corresponding to acquisition times of 120.1 ms in the nitrogen dimension and 75 ms in the proton dimension. The total recording time was 66 h with 16 scans per FID.

Spectra processing was performed with Bruker XWIN-NMR (version 2.6) software. Linear prediction was employed to extend acquisition data in the ^{15}N dimensions (t_2 only) of all 3D experiments by approximately half of their original length. Prior to zero-filling and Fourier transformation, time domain data were apodized with squared-cosine functions in all dimensions. Contour levels of all spectra shown in Figures 2, 4, and 5 are plotted on an exponential scale with a factor of 1.2.

Nitrogen–nitrogen coupling constants were calculated from the ratio of cross-peak and diagonal peak heights according to $J = [\arctan(-I_{cross}/I_{dia})^{1/2}]/\pi\Delta$. By contrast, peak volumes were measured for the evaluation of ^{13}C–^{15}N coupling constants to account for differential line widths of cross-peaks and axial peaks along the ^{13}C dimension in HCN-type quantitative *J*-correlation experiments, caused by faster relaxation of transverse magnetization components that give rise to cross-peaks and by unresolved passive splittings only occurring for the latter.

Acknowledgements

The European Large Scale Facility at the Centre for Biomolecular Magnetic Resonance at the University of Frankfurt is kindly acknowledged for the use of its equipment. We would to thank Dr. Jürgen M. Schmidt (University of Kent at Canterbury) for providing software for volume integration of cross-peaks in 3D spectra. This work was supported by grants from the European Union (QLRT-1999–01003; HPRI-CT-2001-00169; HPRI-CT-2001-50026).

Keywords: flavin · NMR spectroscopy · protein structures · quantitative *J* correlation · TROSY

[1] *Chemistry and Biochemistry of Flavoenzymes*, *Vols.* 1–3 (Ed.: F. Müller), CRC Press, Boca Raton, **1992**.

[2] a) S. G. Mayhew, M. L. Ludwig in *The Enzymes*, *Vol.* 12 (Ed.: P. D. Boyer), Academic Press, New York, **1975**, pp. 57–118; b) R. P. Simondsen, G. Tollin, *Mol. Cell. Biochem.* **1980**, *33*, 13–24; c) S. G. Mayhew, G. Tollin, in *Chemistry and Biochemistry of Flavoenzymes, Vol.* 3 (Ed.: F. Müller), CRC Press, Boca Raton, **1992**, pp. 389–426; d) M. L. Ludwig, C. L. Luschinsky in *Chemistry and Biochemistry of Flavoenzymes, Vol.* 3 (Ed.: F. Müller), CRC Press, Boca Raton, **1992**, pp. 427–466; e) J. Vervoort, D. Heering, S. Peelen, W. van Berkel in *Methods in Enzymology, Vol.* 243 (Eds.: H. D. Peck, Jr., J. LeGall), Academic Press, New York, **1994**, pp. 188–203.

[3] a) R. D. Andersen, P. A. Apgar, R. M. Burnett, G. D. Darling, M. E. LeQuesne, S. G. Mayhew, M. L. Ludwig, *Proc. Natl. Acad. Sci. USA* **1972**, *69*, 3189–3191; b) K. D. Watenpaugh, L. C. Sieker, L. H. Jensen, *Proc. Natl. Acad. Sci. USA* **1973**, *70*, 3857–3860; c) W. W. Smith, R. M. Darling, G. D. Darling, M. L. Ludwig, *J. Mol. Biol.* **1977**, *117*, 195–225; d) W. W. Smith, K. A. Pattridge, M. L. Ludwig, G. A. Petsko, D. Tsernoglou, M. Tanaka, K. T. Yasunobu, *J. Mol. Biol.* **1983**, *165*, 737–755; e) K. Fukuyama, S. Wakabayashi, H. Matsubara, L. J. Rogers, *J. Biol. Chem.* **1990**, *265*, 15804–15812; f) W. Watt, A. Tulinsky, R. P. Swenson, K. D. Watenpaugh, *J. Mol. Biol.* **1991**, *218*, 195–208; g) S. T. Rao, F. Shaffie, C. Yu, K. A. Satyshur, B. J. Stockman, J. L. Markley, M. Sundaralingam, *Protein Sci.* **1992**, *1*, 1413–1427; h) C. T. Sharkey, S. G. Mayhew, T. M. Higgins, M. A. Walsh in *Flavins and Flavoproteins* (Eds.: K. J. Stevenson, V. Massey, C. H. Williams, Jr.), University of Calgary Press, Calgary, **1996**, pp. 445–448; i) A. Romero, J. Caldeira, J. LeGall, I. Moura, J. J. G. Moura, M. J. Romao, *Eur. J. Biochem.* **1996**, *239*, 190–196; j) D. M. Hoover, M. L. Ludwig, *Protein Sci.*

 © 2004 Wiley-VCH Verlag GmbH & Co. KGaA, Weinheim

1997, *6*, 2525 – 2537; k) M. L. Ludwig, K. A. Pattridge, A. L. Metzger, M. M. Dixon, M. Eren, Y. Feng, R. P. Swenson, *Biochemistry* **1997**, *36*, 1259 – 1280; l) M. A. Walsh, A. McCarthy, P. A. O'Farrell, P. McArdle, P. D. Cunningham, S. G. Mayhew, T. M. Higgins, *Eur. J. Biochem.* **1998**, *258*, 362 – 371; m) C. L. Drennan, K. A. Pattridge, C. H. Weber, A. L. Metzger, D. M. Hoover, M. L. Ludwig, *J. Mol. Biol.* **1999**, *294*, 711 – 724; n) J. Freigang, K. Diederichs, K. P. Schäfer, W. Welte, R. Paul, *Protein Sci.* **2002**, *11*, 253 – 261; o) R. Artali, G. Bombieri, F. Meneghetti, G. Gilardi, S. J. Sadeghi, D. Cavazzini, G. L. Rossi, *Acta Cryst. Sect. D* **2002**, *58*, 1787 – 1792.

[4] a) C. P. M. van Mierlo, P. Lijnzaad, J. Vervoort, F. Müller, H. J. C. Berendsen, J. de Vlieg, *Eur. J. Biochem.* **1990**, *194*, 185 – 198; b) B. J. Stockman, A. M. Krezel, J. L. Markley, K. G. Leonhardt, N. A. Straus, *Biochemistry* **1990**, *29*, 9600 – 9609; c) R. T. Clubb, V. Thanabal, C. Osborne, G. Wagner, *Biochemistry* **1991**, *30*, 7718 – 7730; d) B. J. Stockman, T. E. Richardson, R. P. Swenson, *Biochemistry* **1994**, *33*, 15298 – 15308; e) M. Knauf, F. Löhr, M. Blümel, S. G. Mayhew, H. Rüterjans, *Eur. J. Biochem.* **1996**, *238*, 423 – 434; f) S. Peelen, S. S. Wijmenga, P. J. A. Erbel, R. L. Robson, R. R. Eady, J. Vervoort, *J. Biomol. NMR* **1996**, *7*, 315 – 330; g) E. Steensma, N. J. M. Nijman, Y. J. M. Bollen, P. A. de Jager, W. A. M. van den Berg, W. M. A. M. van Dongen, C. P. M. van Mierlo, *Protein Sci.* **1998**, *7*, 306 – 317.

[5] E. Knight, Jr., R. W. F. Hardy, *J. Biol. Chem.* **1966**, *241*, 2752 – 2756.

[6] a) M. Dubourdieu, J. LeGall, *Biochem. Biophys. Res. Commun.* **1970**, *38*, 965 – 972; b) J. M. Odom, H. D. Peck, Jr., *Ann. Rev. Microbiol.* **1984**, *38*, 551 – 592.

[7] a) A. Hvidt, S. O. Nielsen, *Adv. Protein Chem.* **1966**, *21*, 287 – 386; b) G. Wagner, *Q. Rev. Biophys.* **1983**, *16*, 1 – 57; c) S. W. Englander, N. R. Kallenbach, *Q. Rev. Biophys.* **1983**, *16*, 521 – 655.

[8] a) S. N. Loh, J. L. Markley, *Biochemistry* **1994**, *33*, 1029 – 1036; b) A. C. LiWang, A. Bax, *J. Am. Chem. Soc.* **1996**, *118*, 12864 – 12865; c) P. M. Bowers, R. E. Klevit, *Nat. Struct. Biol.* **1996**, *3*, 522 – 531; d) T. K. Harris, A. S. Mildvan, *Proteins: Struct. Funct. Genet.* **1999**, *35*, 275 – 282.

[9] I. Vakonakis, M. Salazar, M. Kang, K. R. Dunbar, A. C. LiWang, *J. Biomol. NMR* **2003**, *25*, *105–112.*

[10] a) C. Wang, X. Gao, R. A. Jones, *J. Am. Chem. Soc.* **1991**, *113*, 1448 – 1450; b) I. Vakonakis, A. C. LiWang, *J. Biomol. NMR* **2004**, *29*, 65 – 72.

[11] a) R. R. Shoup, H. T. Miles, E. D. Becker, *Biochem. Biophys. Res. Commun.* **1966**, *23*, 194 – 201; b) G. Wagner, A. Pardi, K. Wüthrich, *J. Am. Chem. Soc.* **1983**, *105*, 5948 – 5949; c) D. S. Wishart, B. D. Sykes, F. M. Richards, *J. Mol. Biol.* **1991**, *222*, 311 – 333; d) N. E. Zhou, B.-Y. Zhu, B. D. Sykes, R. S. Hodges, *J. Am. Chem. Soc.* **1992**, *114*, 4320 – 4326.

[12] a) N. Tjandra, A. Bax, *J. Am. Chem. Soc.* **1997**, *119*, 8076 – 8082; b) M. Tessari, H. Vis, R. Boelens, R. Kaptein, G. W. Vuister, *J. Am. Chem. Soc.* **1997**, *119*, 8985 – 8990.

[13] a) J. Boyd, T. K. Mal, N. Soffe, I. D. Campbell, *J. Magn. Reson.* **1997**, *124*, 61 – 71; b) A. C. LiWang, A. Bax, *J. Magn. Reson.* **1997**, *127*, 54 – 64.

[14] a) L. Paolillo, E. D. Becker, *J. Magn. Reson.* **1970**, *2*, 168 – 173; b) C. D. Poulter, C. L. Livingston, *Tetrahedron Lett.* **1979**, *9*, 755 – 758; c) N. Jurani , P. K. Ilich, S. Macura, *J. Am. Chem. Soc.* **1995**, *117*, 405 – 410; d) E. L. Ash, J. L. Sudmeier, E. C. DeFabo, W. W. Bachovchin, *Science*, **1997**, *278*, 1128 – 1132.

[15] a) H. D. Franken, H. Rüterjans, F. Müller, *Eur. J. Biochem.* **1984**, *138*, 481 – 489; b) J. Vervoort, F. Müller, J. LeGall, H. Sedlmaier, *Eur. J. Biochem.* **1985**, *151*, 49 – 57; c) J. Vervoort, F. Müller, S. G. Mayhew, W. A. M. van den Berg, C. T. W. Moonen, A. Bacher, *Biochemistry* **1986**, *25*, 6789 – 6799.

[16] a) P. R. Blake, J. B. Park, M. W. W. Adams, M. F. Summers, *J. Am. Chem. Soc.* **1992**, *114*, 4931 – 4933; b) P. R. Blake, B. Lee, M. F. Summers, M. W. W. Adams, J. B. Park, Z. H. Zhou, A. Bax, *J. Biomol. NMR* **1992**, *2*, 527 – 533.

[17] A. J. Dingley, S. Grzesiek, *J. Am. Chem. Soc.* **1998**, *120*, 8293—8297.

[18] K. Pervushin, A. Ono, C. Fernández, T. Szyperski, M. Kainosho, K. Wüthrich, *Proc. Natl. Acad. Sci. USA* **1998**, *95*, 14147 – 14151.

[19] F. Cordier, S. Grzesiek, *J. Am. Chem. Soc.* **1999**, *121*, 1601 – 1602.

[20] G. Cornilescu, J. S. Hu, A. Bax, *J. Am. Chem. Soc.* **1999**, *121*, 2949 – 2950.

[21] A. J. Dingley, J. E. Masse, R. D. Peterson, M. Barfield, J. Feigon, S. Grzesiek, *J. Am. Chem. Soc.* **1999**, *121*, 6019 – 6027.

[22] D. P. Giedroc, P. V. Cornish, M. Hennig, *J. Am. Chem. Soc.* **2003**, *125*, 4676 – 4677.

[23] A. Liu, A. Majumdar, W. Hu, A. Kettani, E. Skripkin, D. J. Patel, *J. Am. Chem. Soc.* **2000**, *122*, 3206 – 3210.

[24] F. Cordier, M. Rogowski, S. Grzesiek, A. Bax, *J. Magn. Reson.* **1999**, *140*, 510 – 512.

[25] A. Meissner, O. Sørensen, *J. Magn. Reson.* **2000**, *143*, 387 – 390.

[26] A. Meissner, O. Sørensen, *J. Magn. Reson.* **2000**, *143*, 431 – 434.

[27] B. Luy, U. Richter, E. S. DeJong, O. W. Sørensen, J. P. Marino, *J. Biomol. NMR* **2002**, *24*, 133 – 142.

[28] F. Cordier, M. Barfield, S. Grzesiek, *J. Am. Chem. Soc.* **2003**, *125*, 15750 – 15751.

[29] a) A. J. Dingley, F. Cordier, S. Grzesiek, *Concepts Magn. Reson.* **2001**, *13*, 103 – 127; b) S. Grzesiek, F. Cordier, A. J. Dingley in *Methods in Enzymology, Vol.* 338 (Eds.: T. L. James, V. Dötsch, U. Schmitz), Academic Press, San Diego, **2001**, pp. 111 – 133; c) S. Grzesiek, F. Cordier, A. J. Dingley in *Biological Magnetic Resonance, Vol.* 20 (Eds.: N. R. Krishna, L. J. Berliner), Kluwer/Plenum, New York, **2003**, pp. 255 – 283; d) A. Dingley, F. Cordier, V. A. Jaravine, S. Grzesiek in *Methods and Principles in Medicinal Chemistry, Vol.* 16 (Ed.: O. Zerbe), Wiley-VCH, Weinheim, **2003**, pp. 207 – 226.

[30] A. Majumdar, D. J. Patel, *Acc. Chem. Res.* **2002**, *35*, 1 – 11.

[31] M. Mishima, S. Hatanaka, S. Yokoyama, T. Ikegami, M. Wälchli, Y. Ito, M. Shirakawa, *J. Am. Chem. Soc.* **2000**, *122*, 5883 – 5884.

[32] F. Löhr, S. G. Mayhew, H. Rüterjans, *J. Am. Chem. Soc.* **2000**, *122*, 9289 – 9295.

[33] A. Liu, A. Majumdar, F. Jiang, N. Chernichenko, W. Skripkin, D. J. Patel, *J. Am. Chem. Soc.* **2000**, *122*, 11226 – 11227.

[34] a) M. A. Knauf, F. Löhr, G. P. Curley, P. O'Farrell, S. G. Mayhew, F. Müller, H. Rüterjans, *Eur. J. Biochem.* **1993**, *213*, 167 – 184; b) B. J. Stockman, A. Euvrad, D. A. Kloosterman, T. A. Scahill, R. P. Swenson, *J. Biomol. NMR* **1993**, *3*, 133 – 149; c) S. Peelen, J. Vervoort, *Arch. Biochem. Biophys.* **1994**, *314*, 291 – 300.

[35] S. G. Mayhew, *Eur. J. Biochem.* **1999**, *265*, 698 – 702.

[36] G. P. Curley, M. C. Carr, S. G. Mayhew, G. Voordouw, *Eur. J. Biochem.* **1991**, *202*, 1091 – 1100.

[37] W. L. DeLano, The PyMOL Molecular Graphics System (2002) DeLano Scientific, San Carlos, CA, USA.

[38] A. Bax, G. W. Vuister, S. Grzesiek, F. Delaglio, A. C. Wang, R. Tschudin, G. Zhu in *Methods in Enzymology, Vol.* 239 (Eds.: T. L. James, N. J. Oppenheimer), Academic Press, New York, **1994**, pp. 79 – 105.

[39] G. N. Yalloway, F. Löhr, H. Rüterjans, S. G. Mayhew in *Flavins and Flavoproteins* (Eds.: S. Chapman, R. Perham, N. Scrutton), Rudolf Weber Agency for Scientific Publications, Berlin, **2002**, pp. 679 – 684.

[40] F. Löhr, H. Rüterjans, *J. Magn. Reson.* **1998**, *132*, 130 – 137.

[41] A. Majumdar, A. Kettani, E. Skripkin, *J. Biomol. NMR* **1999**, *14*, 67 – 70.

[42] G. Cornilescu, B. E. Ramirez, M. K. Frank, G. M. Clore, A. M. Gronenborn, A. Bax, *J. Am. Chem. Soc.* **1999**, *121*, 6275 – 6279.

[43] Y.-X. Wang, J. Jacob, F. Cordier, P. Wingfield, S. J. Stahl, S. Lee-Huang, D. Torchia, S. Grzesiek, A. Bax, *J. Biomol. NMR* **1999**, *14*, 181 – 184.

[44] a) F. Löhr, C. Pérez, J. M. Schmidt, H. Rüterjans, *Bull. Magn. Reson.* **1999**, *20*, 9 – 14; b) F. Löhr, H. Rüterjans, *J. Magn. Reson.* **2000**, *146*, 126 – 131; c) H. L. J. Wienk, M. M. Martínez, G. N. Yalloway, J. M. Schmidt, C. Pérez, H. Rüterjans, F. Löhr, *J. Biomol. NMR* **2003**, *25*, 133 – 145.

[45] a) S. Grzesiek, A. Bax, *J. Am. Chem. Soc.* **1993**, *115*, 12593 – 12594; b) J. Stonehouse, G. L. Shaw, J. Keeler, E. D. Laue, *J. Magn. Reson. Ser. A* **1994**, *107*, 178 – 184; c) H. Matsuo, Ē. Kupče, H. Li, G. Wagner, *J. Magn. Reson. Ser. B* **1996**, *111*, 194 – 198.

[46] A. J. Shaka, P. B. Barker, R. Freeman, *J. Magn. Reson.* **1985**, *64*, 547 – 552.

[47] D. J. States, R. A. Haberkorn, D. J. Ruben, *J. Magn. Reson.* **1982**, *48*, 286 – 292.

[48] G. A. Morris, R. Freeman, *J. Am. Chem. Soc.* **1979**, *101*, 760 – 762.

[49] a) A. Bax, R. H. Griffey, B. L. Hawkins, *J. Magn. Reson.* **1983**, *55*, 301 – 315; b) M. R. Bendall, D. T. Pegg, D. M. Doddrell, *J. Magn. Reson.* **1983**, *52*, 81 – 117.

[50] K. Kawano, N. Ohishi, A. T. Suzuki, Y. Kyogoku, K. Yagi, *Biochemistry* **1978**, *17*, 3854 – 3859.

[51] F.-C. Chang, L. H. Bradley, R. P. Swenson, *Biochim. Biophys. Acta* **2001**, 1504, 319 – 328.

[52] A. Liu, W. Hu, S. Qamar, A. Majumdar, *J. Biomol. NMR* **2000**, *17*, 55 – 61.

[53] R. E. London, *J. Magn. Reson.* **1990**, *86*, 410 – 415.

[54] C. Pérez, F. Löhr, H. Rüterjans, J. M. Schmidt, *J. Am. Chem. Soc.* **2001**, *123*, 7081 – 7093.

[55] G. N. Yalloway, F. Löhr, H. L. J. Wienk, S. G. Mayhew, A. Hrovat, M. A. Knauf, H. Rüterjans, *J. Biomol. NMR* **2003**, *25*, 257 – 258.

 © 2004 Wiley-VCH Verlag GmbH & Co. KGaA, Weinheim

[56] A. Hrovat, M. Blümel, F. Löhr, S. G. Mayhew, H. Rüterjans, *J. Biomol. NMR* **1997**, *10*, 53 – 62.
[57] a) C. Griesinger, O. W. Sørensen, R. R. Ernst, *J. Am. Chem. Soc.* **1985**, *107*, 6394 – 6396; b) G. T. Montelione, M. E. Winkler, P. Rauenbuehler, G. Wagner, *J. Magn. Reson.* **1989**, *82*, 198 – 204.
[58] M. Barfield, A. J. Dingley, J. Feigon, S. Grzesiek, *J. Am. Chem. Soc.* **2001**, *123*, 4014 – 4022.
[59] X. Yan, X. Kong, Y. Xia, K. H. Sze, G. Zhu, *J. Magn. Reson.* **2000**, *147*, 357 – 360.
[60] Z. Wu, A. Ono, M. Kainosho, A. Bax, *J. Biomol. NMR* **2001**, *19*, 361 – 365.
[61] K. Pervushin, C. Fernández, R. Riek, A. Ono, M. Kainosho, K. Wüthrich, *J. Biomol. NMR* **2000**, *16*, 39 – 46.
[62] A. Pardi, G. Wagner, K. Wüthrich, *Eur. J. Biochem.* **1983**, *137*, 445 – 454.
[63] a) C. Scheurer, R. Brüschweiler, *J. Am. Chem. Soc.* **1999**, *121*, 8661 – 8662; b) A. Bagno, *Chem. Eur. J.* **2000**, *6*, 2925 – 2930; c) J. Czernek, R. Brüschweiler, *J. Am. Chem. Soc.* **2001**, *123*, 11 079 – 11 080; d) M. Barfield, *J. Am. Chem. Soc.* **2002**, *124*, 4158 – 4168; e) T. Tuttle, E. Kraka, A. Wu, D. Cremer, *J. Am. Chem. Soc.* **2004**, *126*, 5093 – 5107.
[64] M. A. Walsh, Ph.D. thesis, National University of Ireland, Galway (Ireland), **1994**.
[65] P. A. O'Farrell, M. A. Walsh, A. A. McCarthy, T. M. Higgins, G. Voordouw, S. G. Mayhew, *Biochemistry* **1998**, *37*, 8405 – 8416.
[66] J. Wöhnert, A. J. Dingley, M. Stoldt, M. Görlach, S. Grzesiek, L. R. Brown, *Nucleic Acids Res.* **1999**, *27*, 3104 – 3110.
[67] M. Hennig, B. H. Geierstanger, *J. Am. Chem. Soc.* **1999**, *121*, 5123 – 5126.
[68] A. O. Cuello, C. M. McIntosh, V. M. Rotello, *J. Am. Chem. Soc.* **2000**, *124*, 3517 – 3521.
[69] L. H. Bradley, R. P. Swenson, *Biochemistry* **2001**, *40*, 8686 – 8695.
[70] K. Pervushin, R. Riek, G. Wider, K. Wüthrich, *Proc. Natl. Acad. Sci. USA* **1997**, *94*, 12 366 – 12 371.
[71] a) L. E. Kay, P. Keifer, T. Saarinen, *J. Am. Chem. Soc.* **1992**, *114*, 10 663 – 10 665; b) M. Czisch, R. Boelens, *J. Magn. Reson.* **1998**, *134*, 158 – 160; c) K. Pervushin, G. Wider, K. Wüthrich, *J. Biomol. NMR* **1998**, *12*, 345 – 348; d) J. Weigelt, *J. Am. Chem. Soc.* **1998**, *120*, 10 778 – 10 779.
[72] D. S. Wishart, C. G. Bigam, J. Yao, F. Abildgaard, H. J. Dyson, E. Oldfield, J. L. Markley, B. D. Sykes, *J. Biomol. NMR* **1995**, *6*, 135 – 140.
[73] Ē. Kupče, R. Freeman, *J. Magn. Reson. Ser. A* **1995**, *115*, 273 – 276.
[74] a) R. Fiala, J. Czernek, V. Sklenář, *J. Biomol. NMR* **2000**, *16*, 291 – 302; b) P. Permi, I. Kilpeläinen, A. Annila, *J. Magn. Reson.* **2000**, *146*, 255 – 259; c) F. Löhr, S. Pfeiffer, Y.-J. Lin, J. Hartleib, O. Klimmek, H. Rüterjans, *J. Biomol. NMR* **2000**, *18*, 337 – 346; d) A. Eletsky, A. Kienhofer, K. Pervushin, *J. Biomol. NMR* **2001**, *20*, 177 – 180.
[75] L. Emsley, G. Bodenhausen, *Chem. Phys. Lett.* **1990**, *165*, 469 – 476.
[76] a) J. Boyd, N. Soffe, *J. Magn. Reson.* **1989**, *85*, 406 – 413; b) S. Patt, *J. Magn. Reson.* **1992**, *96*, 94 – 102.

Received: May 25, 2004

 © 2004 Wiley-VCH Verlag GmbH & Co. KGaA, Weinheim